

Direct Synthesis and Mass Spectroscopic Observation of the $\{M_{40}\}$ Polyoxothiometalate Wheel

Haralampos N. Miras,^{*[a]} Hong Ying Zang,^[a] De-Liang Long,^[a] and Leroy Cronin^{*[a]}

Keywords: Molybdenum / Sulfur / Self-assembly / Oxothiometalates

The nanosized, 2.2 nm, $\{Mo_{40}\}$ oxo(thio)metalate wheel was isolated in high yield using a direct synthetic procedure which involves acidification of a molybdate solution in the presence of the $\{Mo_2O_2S_2\}^{2+}$ oxothio cation as the starting material. The $[(Mo_8O_{28})_4(Mo_2O_2S_2)_4]^{24-}$ wheel, **1a**, was characterised by single-crystal X-ray diffraction analysis, IR, Raman, UV/Vis and flame atomic absorption spectroscopy (FAAS). Solid state and solution Raman spectroscopic studies allowed the unambiguous determination of the critical conditions by which compound **1** retains its integrity in solution.

Electrospray ionisation mass spectrometry (ESI-MS) studies carried out on aqueous solutions of the crystalline material showed that the nanosized wheel retains its integrity in concentrated solutions. High resolution ESI-MS studies allowed the direct observation of the discrete wheel as well as the distinct self-assembly stages of its formation; from the fundamental building units through to the final formation of well resolved aggregations of 1D chains which is in agreement with the solid state studies.

Introduction

The great interest in polyoxometalates (POMs) reflects the diverse nature of this family of inorganic clusters^[1] which exhibit a wide variety of compositions and architectures^[2] as well as important optical,^[3] catalytic^[4] and magnetic^[5] properties. Consequently, the observed properties of this class of materials are directly related to their architecture and composition. In this context, the chemistry of tungstates^[6] and molybdates^[7] is unmatched since it allows “selection” rules to be applied to a diverse library of molybdenum and tungsten oxide based synthons for the design of unprecedented architectures. More specifically, the condensation process of aqueous molybdate solutions can lead to the formation of a plethora of anionic species with sizes spanning from 1.0 to 5.6 nm and shapes ranging from Keggin $[XMo_{12}O_{42}]$ structures to nanosized spheres, rings and “lemon” shaped architectures.^[8] The long list of the aforementioned “selection” rules such as the “shrink-wrapping” effect of weakly chelating ligands, reducing environment, metallic cations, heteroanions, ionic strength, flow conditions etc.,^[9] direct the stabilisation of unique sets of building blocks which further on can be assembled towards the formation of discrete nanosized moieties.^[9a,10]

On the other hand, oxothiometalates constitute a subclass of the POM family which consists of considerably fewer members. The polyoxothiometalates (POTM) bear little resemblance to their oxo-based analogues due to the fact that the sulfide ion is larger than the oxide, is a poorer π donor and easier to get oxidized.^[11] Although a large number of thio- and oxothiomolybdates have been reported in the literature,^[12] most of these compounds are structurally based on conventional architectures of low nuclearity ranging from the mononuclear anion, $[MoO_{4-n}S_n]^{2-}$ to tetranuclear oxothiomolybdates such as the dimeric $\{Mo_4O_4S_{14}\}^{2-}$ species^[13] or in the cubane like cluster $[Mo_4S_4(CN)_{12}]^{5-}$.^[14] The first step for the preparation of these compounds usually involves a direct sulfurisation process to provide thioanions which are precursors for more sophisticated species by means of reactions with electrophiles (H^+ or Cu^{2+})^[15] or nucleophiles (cyanido or trialkylphosphane).^[16–18] The last decade though has given a plethora of unprecedented architectures with interesting properties^[19] expanding the limited family of POTM-based compounds because of the fruitful efforts of Sécheresse, Cadot, Dolbecq et al.

Herein we report the direct preparation method of the nanosized oxothiometalate $\{Mo_{40}\}$ wheel, $[(Mo_8O_{28})_4(Mo_2O_2S_2)_4]^{24-}$ **1a**, previously described by Cadot et al.^[20a] We also describe the observation, by high resolution electrospray ionization mass spectrometry (ESI-MS), of the discrete as well as the dimeric species of **1** formed in solution. In this new method, we employed the discrete $\{Mo_2O_2S_2\}^{2+}$ oxothio cation as the inorganic linker in the presence of a molybdenum source to give the desirable product in considerably improved yield for such a big architecture. The

[a] School of Chemistry, The University of Glasgow, Glasgow, G12 8QQ, UK
Fax: +44-141-330-4888
E-mail: harism@chem.gla.ac.uk
l.cronin@chem.gla.ac.uk
Homepage: <http://www.croninlab.com>

Supporting information for this article is available on the WWW under <http://dx.doi.org/10.1002/ejic.201100833> or from the author.

mentioned synthetic method simplifies the formation of the $\{\text{Mo}_{40}\}$ wheel in one single step under mild conditions (room temperature) obtaining good yields which makes it energetically more favourable and less time consuming. The cluster has been characterised extensively in solid state by X-ray diffraction studies, FAAS, IR and Raman spectroscopy as well as in solution by ESI-MS studies and Raman spectroscopy. Furthermore, high-resolution ESI-MS studies on the reaction mixtures revealed the formation and demonstrated the structural integrity of the fundamental synthon, $\{\text{Mo}_8\text{O}_{28}\}$, in solution.

Results and Discussion

The nanosized oxothiometalate $[(\text{Mo}_8\text{O}_{28})_4(\text{Mo}_2\text{O}_2\text{S}_2)_4]^{24-}$ was prepared by treatment of $\text{Na}_2\text{MoO}_4 \cdot 2\text{H}_2\text{O}$ with $\{\text{Mo}_2\text{O}_2\text{S}_2\}^{2+}$ in a reducing environment in a sodium acetate solution. Despite the fact that the successful original synthesis reported by Cadot et al. involves the use of the cyclic compound $\text{K}_2\text{I}_2[\text{Mo}_{10}\text{O}_{10}\text{S}_{10}(\text{OH})_{10}(\text{H}_2\text{O})_5] \cdot 15\text{H}_2\text{O}$ as an additional Mo source followed by heating the mixture at 40 °C, we envisaged that the synthetic procedure could potentially be improved in terms of yield of the isolated product and be energetically more efficient and less time consuming by being carried out in a one pot procedure at room temperature. It is well known that oxothiometalates are susceptible to oxidation and, consequently, to disintegration of the architecture under specific conditions. Based on the initial synthesis reported by Cadot et al., heating a solution containing the $\{\text{Mo}_{10}\}$ ring precursor at 40 °C promotes the decomposition of the cluster to its building units $\{\text{Mo}_2\text{O}_2\text{S}_2\}^{2+}$ which were used further during the following step of the synthetic procedure. Furthermore, under the described conditions, partial oxidation of the μ_2 -sulfur bridges within the dimer takes place and induces fragmentation of the useful dimeric $\{\text{Mo}_2\text{O}_2\text{S}_2\}^{2+}$ unit which consequently should lead to decreased yield. Based on the above observations, we envisaged an alternative direct synthetic route which should lead to higher yield, isolation of better quality single crystals as well as to an improved understanding of the underlying chemistry of the system. More specifically, the synthetic procedure we followed involved the reaction under mild conditions at room temperature of a $\text{Na}_2\text{MoO}_4 \cdot 2\text{H}_2\text{O}$ aqueous solution with the presynthesised dimeric unit $\{\text{Mo}^{\text{V}}\text{O}_2\text{S}_2\}^{2+}$ giving a solution with a pH value of 5. At this point an amount of reducing agent was added immediately to the reaction mixture in order to prevent intramolecular redox processes from taking place between the Mo^{VI} centres and the oxidation sensitive $\{\text{Mo}^{\text{V}}\text{O}_2\text{S}_2\}^{2+}$ unit. The addition of the reducing agent further inhibited the formation of the very stable $\{\text{Mo}_9\}$ ^[20b] ring which shifts the position of equilibrium in a completely undesirable direction. By protecting the dimeric $\{\text{Mo}^{\text{V}}\text{O}_2\text{S}_2\}^{2+}$ species from any wanted redox side-reactions which could lead to disintegration of the building unit, we were able to adjust the pH to the desired value of 4.2 without encountering problems due to the formation of byprod-

ucts such as the very stable $\{\text{Mo}_9\}$ thiometalate ring, the self-assembly of which is well known to be favoured in very high yields below the crucial pH value of 5.^[20b] The solution was buffered using sodium acetate in order to prevent pH changes during the crystallisation period which might affect the yield and/or the nature of the isolated product. Moreover, the increased ionic strength of the solution helped us isolate single crystals of improved quality in a relatively short period of time as has been observed before in POM-based systems by our group and others.^[9] Interestingly, the use of a reducing environment did not seem to affect the oxidation state of the metal centres in the isolated material as has been proven by charge balance considerations, elemental analyses and bond valence sum (BVS) calculations. This is an additional indication that the role of the reducing environment is to prevent the oxidation of the fundamental dimeric building units in solution as well as to inhibit the formation of the very stable $\{\text{Mo}_9\}$ species, since the system has the tendency to become oxidised easily even under mild conditions. In order to verify the validity of the above observation, we tried to synthesise the material in the absence of a reducing agent without success even if we degassed the solutions prior to reaction and kept the crystallisation flasks sealed. Instead, a mixture of $\{\text{Mo}_9\}$, elemental sulfur and a quantity of an unidentified light brown precipitate was isolated.

Compound **1**, isolated as dark brown single crystals of a mixed sodium-potassium salt from a solution with a resultant pH of 4.2, was characterised by single-crystal X-ray structural analysis at low temperature (150 K), elemental and thermogravimetric analysis (TGA; Figure S2 in the Supporting Information), FTIR, UV/Vis reflectance (Figures S1 and S3) and Raman spectroscopy (Figure 5). Furthermore, the material was studied extensively in solution by high resolution ESI mass spectrometry where a direct observation of the nanosized wheel along with the evolution of the 1D polymer chains was carried out while stability studies were conducted as a function of the concentration of compound **1** by utilising ESI-MS and Raman spectrometry (see below). A selection of interatomic distances and bond angles relevant to the molybdenum coordination spheres for compound **1** is listed in Tables 1 and 2. **1a** exhibits an idealised C_{4v} symmetry and crystallises in the space group $C2/m$ and has unit cell parameters of $a = 23.1173(5)$, $b = 25.5430(5)$ and $c = 37.3809(7)$ Å and a unit cell volume of 21891.1(8) Å³. Isolating high quality single-crystals of compound **1** and collecting X-ray data at the low temperature of 150 K allowed us to obtain structural information at a higher resolution, minimising, and in most cases eliminating, disorder problems with solvent molecules and counterions and finally achieving an R value of 0.074 (see Table 3). The structure solution revealed the thiometalate nanoscale $\{\text{Mo}_{40}\}$ wheel, with an external diameter of 2.2 nm, constructed from four new $\{\text{Mo}_8\text{O}_{28}\}^{8-}$ species connected together by four dimeric $\{\text{Mo}^{\text{V}}\text{O}_2\text{S}_2\}^{2+}$ units. It is worth pointing out that the $\{\text{Mo}_8\}$ species was observed for the first time in an acidified molybdenum solution, revealing a potential for future design and development of new

high nuclearity architectures. The {Mo₈} oxo building blocks can be described as two half Mo-cubanes, {Mo₃O₁₃}, connected together through a Mo-dimer bridge, {Mo₂}, by means of two corner-shared octahedra. The resultant building block, {Mo₈O₂₈}⁸⁻ (Figure 2), consists of eight molybdenum centres which describe an octahedral geometry at their highest oxidation state, Mo^{VI}, with one or two terminal metal-oxo bonds completing their coordination sphere. All the oxygen atoms found to be deprotonated according to the bond valence sum calculation (BVS) studies conducted for all the atoms. The {Mo^{VI}₈O₂₈}⁸⁻ blocks are connected further together by {Mo^V₂O₂S₂}²⁺ linkers in a cyclic fashion as shown in Figure 1.

Table 1. Selected interatomic distances relevant to the coordination sphere of molybdenum atoms for compound **1**.

Bond lengths / Å			
Mo1–O21	1.68(1)	Mo18–O75	1.68(2)
Mo2–O14	1.68(2)	Mo19–O55	1.68(1)
Mo3–O37	1.70(1)	Mo20–O44	1.69(2)
Mo4–O20	1.70(1)	Mo21–O79	1.72(2)
Mo5–O16	1.66(1)	Mo22–O90	1.70(2)
Mo7–O40	1.70(1)	Mo5–S1	2.271(5)
Mo8–O42	1.70(1)	Mo5–S2	2.266(5)
Mo9–O28	1.72(1)	Mo16–S3	2.242(7)
Mo10–O33	1.68(1)	Mo16–S4	2.226(8)
Mo11–O32	1.70(1)	Mo18–S3	2.254(8)
Mo12–O38	1.70(1)	Mo18–S4	2.256(7)
Mo13–O49	1.69(1)	Mo10–S1	2.245(5)
Mo14–O31	1.71(2)	Mo10–S2	2.253(5)
Mo15–O73	1.69(1)	Mo5–Mo10	2.759(2)
Mo16–O71	1.67(2)	Mo16–Mo18	2.734(2)
Mo17–O53	1.70(2)		

Table 2. Selected angles relevant to the coordination sphere of molybdenum and sulfur atoms for compound **1**.

Bond angles / °			
Mo10–Mo5–S1	51.9(1)	S3–Mo16–S4	100.6(3)
Mo10–Mo5–S2	52.2(1)	Mo16–Mo18–S3	52.3(2)
S1–Mo5–S2	100.8(2)	Mo16–Mo18–S4	51.9(2)
Mo5–Mo10–S1	52.8(1)	S3–Mo18–S4	99.3(3)
Mo5–Mo10–S2	52.6(1)	Mo5–S1–Mo10	75.3(2)
S1–Mo10–S2	102.0(2)	Mo5–S2–Mo10	75.3(2)
Mo18–Mo16–S3	52.7(2)	Mo16–S3–Mo18	74.9(3)
Mo18–Mo16–S4	52.9(2)	Mo16–S4–Mo18	75.2(3)

The wheels are further connected together by sodium and potassium cations in an overall 1D chain architecture (Figure S4). The distribution of the Mo–μ₂–O–Mo and Mo–μ₃–O–Mo angles within the {Mo₈} cluster spans from 114.1(4)° to 122.6(7)° and 92.0(5)° to 145.0(8)°, respectively. Each of the {Mo₈} units in **1** contains five molybdenum atoms with two terminal O atoms with average Mo=O and Mo–O bond lengths of 1.73(2) and 2.12(3) Å, respectively. Furthermore, each of the {Mo₈} units can be considered as lacunary species which represent two symmetric coordination sites available for the two {Mo₂O₂S₂}²⁺ linkers, see Figure 2. The bond lengths and angles within the {Mo₂O₂S₂}²⁺ linkers have values Mo^V–Mo^V = 2.75(2) Å, Mo^V–S = 2.25(2) Å and Mo–O_t = 1.67(2) Å. These are comparable to the previously reported examples.^[11c,12] The

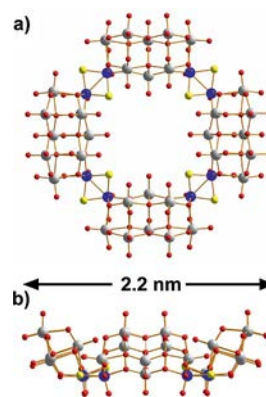


Figure 1. a) “Ball-and-stick” representation of the {Mo₄₀} wheel **1a** (colour code: red, O; yellow, S; Mo atoms in {Mo₈O₂₈}⁸⁻ unit, grey; Mo in {Mo₂O₂S₂}²⁺ unit, blue). b) Side view of **1a** in “ball-and-stick” representation.

length distribution of the equatorial Mo^V–O bonds within the Mo^V–O–Mo^{VI} bridges, represent an average length of [2.20(2) Å] while the oxo bridges located in *trans* position to the Mo^{VO}_t bonds, lie [2.36(1) Å] far away from the molybdenum centres, respectively.

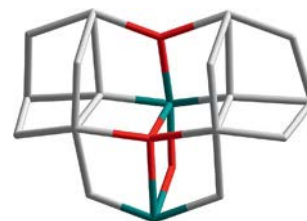


Figure 2. Wire-frame representations of the {Mo₈O₂₈}⁸⁻ building block within **1** showing the bridging of the two half-cubane units by means of a {Mo₂} bridge. (colour code: red, O; {Mo₂} unit, green; half-cubane units, grey).

ESI-MS Studies

The ESI-MS technique has proved to be a very diverse and informative technique in polyoxometalate chemistry,^[21] providing very important information regarding a compound's structural integrity in solution,^[22,9c] its composition,^[23,9b] the extent of protonation^[24,9b] and it can unveil the formation mechanism which takes place during the self-assembly process.^[25] In an effort to investigate the wheel's behaviour in solution, we conducted high resolution ESI-MS studies by which we managed to directly observe not only the intact wheel but the existence of its building units as well as the gradual formation of the 1D chains in solution which is in agreement with solid-state studies by X-ray diffraction analysis. Consideration of low *m/z* values unveiled a –2 charged species which can be assigned unambiguously to the fundamental synthon of the wheel shaped architecture and can be formulated as {K₄[(Mo₈O₂₈)-(Mo₂S₂O₂)](H₂O)₄}²⁻, see Figure 3.

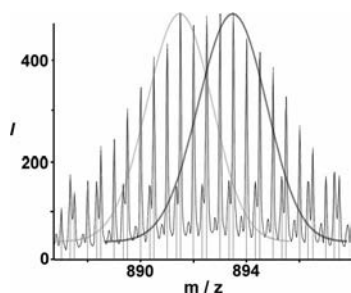


Figure 3. Negative ion mass spectrum in aqueous solution of $\{K_{(1+n)}NaH_{(2-n)}[(Mo_8O_{28})(Mo_2S_2O_2)](H_2O)_{(12-2n)}\}^{2-}$. Two envelopes can be seen where $n = 0$ (two fold protonated) giving an envelope centred at m/z ca. 891.97 and where $n = 2$ (deprotonated species) giving an envelope centred at m/z ca. 893.90. Black line: experimental data, red/blue lines: profile lines of the simulated isotopic patterns.

The direct observation of the building units which make up the nanosized architecture is very important since it shows that the unprecedented $\{Mo_8\}$ synthon is stable enough in solution to react with electrophiles of appropriate geometry and assemble to form large architectures. On the other hand, investigation of the high m/z region unveiled a series of isotopic distribution envelopes assignable to species representing different degrees of protonation and hydration (Figure 4). Interestingly, it was possible to observe the discrete molecule as well as stages involved in the assembly of the 1D chains (Figure 4).

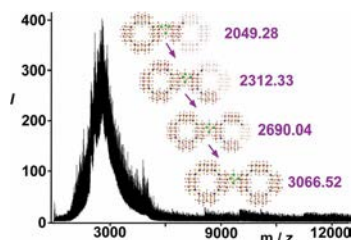


Figure 4. High m/z region of the spectrum of an aqueous solution of **1** in negative ion mode. A series of isotopic distribution envelopes observed due to different degrees of protonation and hydration. A gradual evolution of the 1D chain detected giving separate envelopes centred at m/z ca. 2049.28, 2312.33, 2690.04 and 3066.52. For detailed analysis of the individually observed envelopes and assignment of the observed species, see figures S5–S15 in the ESI.

The ability to observe discrete nanosized molecules and follow their assembly into larger formations unveils crucial information related to their relevant stability under specific experimental conditions,^[9c,22] their formation mechanism^[25] as well as the availability and stability of a fundamentally novel set of synthons. In this case the observation of the unique $\{Mo_8\}$ synthon in the solid state as well as in solution is quite intriguing since this unit offers unlimited possibilities for the further design and construction of nanosized architectures with a wide range of functionalities. Since, during the ESI-MS studies, partial fragmentation of the species might occur (specifically when we deal with fragile architectures), it is then possible to transmit many of the

labile species present in solution into the mass spectrometer and allow correlation of the observed data with possible mechanisms of fragmentation of the compounds which can then be compared and contrasted with tentative ideas regarding the assembly of the clusters. In this respect, it is vital to point out that ESI-MS studies on nanosized inorganic frameworks in aqueous media are intrinsically lacking with regards to mechanistic information for self-assembly but, at the same time, such data may be useful for comparing and contrasting with direct observations of the solutions of the materials. Furthermore, the information yielded can be useful for at least postulating some ideas that could then be used to form testable hypotheses.

It is worth pointing out at this time that the ESI-MS studies were conducted in relatively concentrated solutions of **1** ($\approx 5 \times 10^{-2} \text{ mol L}^{-1}$). In an effort to monitor the stability of the wheel by utilising the ESI-MS technique, we realised that it was possible to record a mass spectrum of sufficient quality only for concentrations higher than 10^{-2} M in aqueous media. This observation is in agreement with the UV/Vis spectroscopic studies in solution conducted by Cadot et al. as well as the solution Raman spectroscopic studies carried out at different concentrations and a comparison with the spectrum obtained in solid state is possible (see below).

Spectroscopic Studies

The IR spectrum of the $\{Mo_{40}\}$ ring was recorded using a KBr pellet (Figure S1). The observed peaks were assigned based on the structural features of **1** and found to be in good agreement with previously reported thiometalate rings in the literature.^[26–29] The peak at 1618 (m) can be assigned to H_2O molecules in the crystal lattice. Accordingly, the peaks at 943 (s), 865 (s) and 823 (w) can be assigned to the stretching vibrations of the $Mo=O$, $Mo-O$ and $Mo-S$, respectively. Finally the group of peaks at 781 (w), 726 (s) and 643 (vs) arise from the $Mo-O-Mo$ bending vibrations while the weaker ones at 479 (w) and 420 (w) can be assigned to the $Mo-S-Mo$ bending vibrations, respectively.

The oxothiometalate compound was studied by Raman spectroscopy in the solid state as well as in solution in order to determine its stability in aqueous media at various concentrations. The solid state Raman spectra, as shown in Figure 5, exhibit characteristic bands due to the terminal $Mo=O$. The corner $Mo-O-Mo$ and the three-coordinate edge OMo_3 oxygen–molybdenum stretching vibrations appear at 949, 904, 867 and 701 cm^{-1} , respectively.^[30–33] Bands due to the terminal, corner $Mo-O-Mo$, $Mo-S-Mo$ and three-coordinate edge OMo_3 oxygen–molybdenum bending vibrations appear in the same region at 488, 351 and 198 cm^{-1} , respectively.^[30–32]

In addition to the solid state characterisation, the thiometalate ring was studied in solution using Raman spectroscopy at different concentrations of compound **1**. As shown in Figure 6, the nanosized ring is relatively stable in concentrated solutions, $> 10^{-2} \text{ M}$, while at concentrations $<$

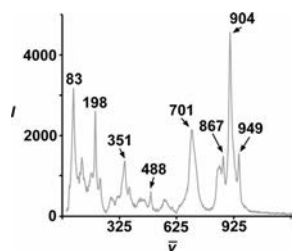


Figure 5. Raman spectrum of crystalline sample of **1**.

10^{-3} M it seems to decompose rapidly (≈ 10 min) which consequently causes a decrease in the intensity of the characteristic peaks of the material. The aforementioned observation was verified by ESI-MS studies in which we were unable to detect the intact ring shaped architecture of the $\{Mo_{40}\}$ oxothiometalate at concentrations lower than 10^{-2} M.

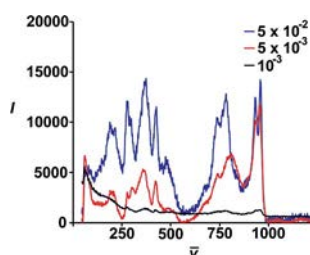


Figure 6. Raman spectrum of **1** in aqueous solution at different concentrations. Decomposition of dilute solutions of **1** was detected after approximately 10 min.

In every case, the main features of the spectra are located in the region $800\text{--}1000\text{ cm}^{-1}$ due to $Mo=O$ (sym./asym.) at higher frequencies and to $Mo-O-Mo$ and $Mo-S-Mo$ (sym) at lower frequencies.^[26] Moreover, a minor broadening of the bands was observed in the case of the spectra which were recorded in aqueous media and this is due to the existence of an extensive network of hydrogen bonds between the nanosized ring, the potassium/sodium counterions and solvent molecules. Similar behaviour has been observed before in which proton induced polarisabilities contribute to the electron based ones causing a broader distribution of accessible energy levels.^[34–36]

As an extension of the detailed UV/Vis spectroscopic solution studies reported by Cadot et al.,^[20a] which are in good agreement with our spectroscopic studies in solution and the solid state, we recorded the UV/Vis reflectance spectra (Figure S3) which gives us unambiguous proof of the electronic structure of **1** and assists further in the direct comparison of the data obtained from solution and the solid state. Three overlapping broad shoulders can be observed with their maxima located at 450, 350 and 275 nm. The absorption bands can be assigned to charge-transfer transitions of the types $S \rightarrow d(Mo)$ and $O \rightarrow d(Mo)$ (since there is almost no “mixing” between S and O functions).^[11] The reflectance spectrum is in good agreement with the related one collected on a solution^[13] giving us additional proof of the critical concentration above which the thiometalate compound retains its integrity in aqueous media.

Conclusions

In this work we have reported a direct, fast and energetically efficient synthetic procedure for the synthesis of the $\{Mo_{40}\}$ oxothiometalate wheel in improved yield. This involves acidification of a molybdate solution in the presence of the $\{Mo_2O_2S_2\}^{2+}$ oxothio cation as the starting material in a reducing environment. The experimental variables which affect the self-assembly of the nanosized $\{Mo_{40}\}$ wheel were studied and discussed in detail. The reducing environment promotes the stability of the fundamental synthons in solution allowing us to direct the self-assembly towards the desirable outcome which is the formation of the $\{Mo_{40}\}$ wheel whilst, at the same time, avoiding formation of very kinetically stable products such as the $\{Mo_9\}$ species. The isolated crystalline material was characterised extensively in solid state by IR, Raman and UV/Vis reflectance spectroscopy, elemental and FAAS analyses and BVS calculations were undertaken. High resolution X-ray diffraction analysis at low temperature (150 K) was carried out, allowing us to collect high accuracy and quality data giving a final R value of 0.074. Furthermore, high resolution ESI-MS, Raman and UV/Vis spectroscopic studies allowed us to characterise the aforementioned nanosized material in solution at different concentrations allowing a comparison to be done between the relevant data obtained on the solid state structure and this helped us to bridge the gap between the solution and solid state structures and elucidate the critical concentration up to which the $\{Mo_{40}\}$ unit retains its integrity in solution. Furthermore, direct observation of the nanosized architectures in aqueous media is of great importance since it provides additional information regarding the available library of building units in solution while unveiling crucial information to help us at least postulate some ideas that could then be used to form testable hypotheses in regards to the formation mechanism of such complicated chemical systems. Finally, the observation of the unprecedented $\{Mo_8\}$ species in solution is very important since it demonstrates its relevant stability under the experimental conditions and this opens the door for further exploration and design of new materials with potentially intriguing properties.

Experimental Section

Physical Measurements: The materials were prepared as KBr pellets and FTIR spectra were collected in transmission mode using a JASCO FTIR 4100 spectrometer. Wavenumbers (ν) are given in cm^{-1} ; intensities as denoted as w = weak, sh = sharp, m = medium, br. = broad, s = strong. UV/Vis spectra were collected using a JASCO V-670 spectrometer equipped with an ISV723 60 mm integrating sphere in diffuse reflectance mode. Thermogravimetric analyses were performed on a TA Instruments Q 500 Thermogravimetric Analyser under N_2 flow at a typical heating rate of $5\text{ }^\circ\text{C min}^{-1}$. FAAS was performed at the Environmental Chemistry Section, Department of Chemistry, University of Glasgow on a Perkin-Elmer 1100B Atomic Absorption Spectrophotometer whereas carbon, nitrogen and hydrogen content were determined by the microanalysis services within the School of Chemistry, University of Glasgow

using a EA 1110 CHNS, CE-440 Elemental Analyser. The Raman spectra were obtained from a micro-crystalline powder of compound **1** and collected using a HORIBA spectrometer equipped with a green ion laser operating at 532 nm.

ESI-MS Spectroscopy: ESI measurements were carried out at 180 °C. The solutions of the sample were diluted so that the maximum concentration of the cluster ions was of the order of 10^{-1} to 10^{-2} M and the solutions were infused into the electrospray at $180 \mu\text{L h}^{-1}$. The mass spectrometer used for the measurements was a Bruker microTOF-Q and the data were collected in negative ion mode. The spectrometer was previously calibrated with the standard tune mix to give a precision of ca. 1.5 ppm in the region of 500–5000 *m/z*. The standard parameters for a medium mass data acquisition were used and the end plate voltage was set to –500 V and the capillary to –4500 V. The collision cell was set to a collision energy of $-9.0 \text{ eV } z^{-1}$ with a gas flow rate at 25% of maximum and the cell RF was set at 2000 V_{pp} . The predicted spectrum was calculated by using Bruker Data Analysis 3.4 software and was performed by calculating the predicted distribution of the cluster anion.

Synthesis: The dimeric $[\text{Mo}_2\text{S}_2\text{O}_2]^{2+}$ unit was synthesised according to the modified published procedure by E. Cadot et al.^[11d] Iodine (9 g, 35.4 mmol) and KI (16 g, 96.3 mmol) were dissolved in hydrochloric acid (70 mL, 1 M). Then, $(\text{NMe}_4)_2[\text{Mo}_2\text{O}_2\text{S}_6]^{[37]}$ (10 g, 17.7 mmol) was suspended in an aqueous solution of KI (60 mL, 0.7 M) and the iodine solution was slowly added to the suspension with vigorous stirring. The resultant solution was heated to 50 °C for 10 min. The insoluble material formed (mainly solid sulfur and tetramethylammonium iodide) was removed by filtration. The red filtrate was cooled to 0 °C to complete the precipitation of the remaining tetramethylammonium iodide and after filtration the obtained $[\text{Mo}_2\text{O}_2\text{S}_2]^{2+}$ solution was stored under Ar. The purity of the intermediate products was confirmed by FTIR spectroscopy. All other materials were purchased from Sigma Aldrich Chemicals and used without further purification.

$\text{Na}_7\text{K}_{17}[(\text{Mo}_8\text{O}_{28})_4(\text{Mo}_2\text{S}_2\text{O}_2)_4] \cdot 45\text{H}_2\text{O}$: $\text{Na}_2\text{MoO}_4 \cdot 2\text{H}_2\text{O}$ (4.0 g, 16.5 mmol) and CH_3COONa (5.0 g, 60.0 mmol) were dissolved in water (50 mL). To the resultant clear solution was added a solution of $[\text{Mo}_2\text{S}_2\text{O}_2]^{2+}$ dropwise until the pH was adjusted to a value of 5. Addition of $\text{Na}_2\text{S}_2\text{O}_4$ (0.12 g, 0.68 mmol) followed, accompanied by an immediate colour change of the solution to dark green-brown. The pH was adjusted to the value of 4.2 by addition of conc. HCl. The mixture was stirred for 30 min while the solution's colour turned to dark brown and a small amount of precipitate formed. The solution was filtered and the filtrate left in an open vessel at room temperature (≈ 18 °C) for 3 d, during which time deep red-brown crystals suitable for X-ray structure analysis were obtained; yield 1.48 g (48% based on Mo). $\text{H}_{90}\text{K}_{17}\text{Mo}_{40}\text{Na}_7\text{O}_{165}\text{S}_8$ (7650.29); calcd. K 8.69, Na 2.10, Mo 50.16, S 3.35; found K 8.33, Na 1.90, Mo 50.90, S 3.49.

Single Crystal X-ray Diffraction: Details of data collection procedures and structure refinements are given in Table S1. A single crystal of suitable size was attached to glass fibre using Fomblin YR-1800 oil and mounted. The sample was glued to a glass fibre and transferred as rapidly as possible into the cold stream of the Oxford Instruments Cryostream. All data were collected on an Oxford Gemini CCD diffractometer, equipped with graphite-monochromated Cu X-radiation ($\lambda = 1.5418 \text{ \AA}$) at 150 K. The structures were solved by SHELXS-97.^[38] Most of the nonhydrogen atoms were refined anisotropically. The refinement was carried out with SHELXL-97^[39] using full-matrix least-squares on F^2 and all the unique data. The sample showed the presence of disordered solvent

molecules. All calculations were carried out using the WinGX^[40] package of crystallographic programs (Table 3).

Table 3. Crystallographic data collection, intensity measurements and structure refinement parameters for compound **1**.

1	
Chemical formula	$\text{H}_{90}\text{K}_{17}\text{Mo}_{40}\text{Na}_7\text{O}_{165}\text{S}_8$
<i>M</i> [g mol^{-1}]	7650.43
Symmetry	monoclinic
Space group	<i>C2/m</i>
<i>a</i> [\AA]	23.1173(5)
<i>b</i> [\AA]	25.5430(5)
<i>c</i> [\AA]	37.3809(7)
α [$^\circ$]	90
β [$^\circ$]	97.358(2)
γ [$^\circ$]	90
<i>V</i> [\AA^3]	21891.1(8)
<i>T</i> [K]	150(2)
<i>Z</i>	4
μ [mm^{-1}]	22.690
Crystal size [mm]	0.13 × 0.12 × 0.10
Number of data measured	17297
Number of unique data	11299
<i>R</i> ₁	0.0742
<i>wR</i> ₂ (all data)	0.2369
Goof	1.031

Further details on the crystal structure investigation may be obtained from the Fachinformationszentrum Karlsruhe, 76344 Eggenstein-Leopoldshafen, Germany (fax: +49-7247-808-666; e-mail: crysdata@fiz-karlsruhe.de), on quoting the depository number CSD-422644.

Supporting Information (see footnote on the first page of this article): FTIR, TGA and UV/Vis spectroscopic data, additional figures illustrating the crystal structure and details of ESI-MS data.

Acknowledgments

This work was supported by the Engineering and Physical Sciences Research Council (ESPRC), WestCHEM, Royal Society of Edinburgh, Marie Curie Actions and the University of Glasgow.

- [1] a) D.-L. Long, E. Burkholder, L. Cronin, *Chem. Soc. Rev.* **2007**, *36*, 105–121; b) L. Cronin, in: *Comprehensive Coordination Chemistry II* (Eds.: J. A. McCleverty, T. J. Meyer), Elsevier, Amsterdam, **2004**, vol. 7, pp. 1–57; c) D.-L. Long, R. Tsunashima, L. Cronin, *Angew. Chem. Int. Ed.* **2010**, *49*, 1736–1758.
- [2] a) M. T. Pope, A. Müller, *Angew. Chem.* **1991**, *103*, 56; *Angew. Chem. Int. Ed. Engl.* **1991**, *30*, 34–48; b) L. Cronin, *Angew. Chem.* **2006**, *118*, 3656; *Angew. Chem. Int. Ed.* **2006**, *45*, 3576–3578; c) L. Cronin, P. Kögerler, A. Müller, *J. Solid State Chem.* **2000**, *152*, 57–67.
- [3] T. Yamase, *Chem. Rev.* **1998**, *98*, 307–326.
- [4] a) A. Proust, R. Thouvenot, P. Gouzerh, *Chem. Commun.* **2008**, 1837–1852; b) N. Mizuno, M. Misono, *Chem. Rev.* **1998**, *98*, 199–218; c) M. Sadakane, E. Steckhan, *Chem. Rev.* **1998**, *98*, 219–237.
- [5] a) J. M. Clemente-Juan, E. Coronado, *Coord. Chem. Rev.* **1999**, *193–195*, 361–394 and references cited therein; b) C. Ritchie, A. Ferguson, H. Nojiri, H. N. Miras, Y. F. Song, D. L. Long, E. Burkholder, M. Murrie, P. Kögerler, E. K. Brechin, L. Cronin, *Angew. Chem.* **2008**, *120*, 5691; *Angew. Chem. Int. Ed.* **2008**, *47*, 5609–5612.
- [6] a) C. Schäffer, A. Merca, H. Bögge, A. M. Todea, M. L. Kistler, T. Liu, R. Thouvenot, P. Gouzerh, A. Müller, *Angew.*

- Chem.* **2009**, *121*, 155; *Angew. Chem. Int. Ed.* **2009**, *48*, 149–153; b) S. Reinoso, M. Giménez-Marqués, J. R. Galán-Mascarós, P. Vitoria, J. M. Gutiérrez-Zorrilla, *Angew. Chem. Int. Ed.* **2010**, *49*, 8384–8388; c) J. Yan, J. Gao, D.-L. Long, H. N. Miras, L. Cronin, *J. Am. Chem. Soc.* **2010**, *132*, 11410–11411.
- [7] a) P. Kögerler, L. Cronin, *Angew. Chem.* **2005**, *117*, 866; *Angew. Chem. Int. Ed.* **2005**, *44*, 844–846; b) C. Ritchie, E. Burkholder, P. Kögerler, L. Cronin, *Dalton Trans.* **2006**, 1712–1714; c) D.-L. Long, P. Kögerler, L. J. Farrugia, L. Cronin, *Angew. Chem.* **2003**, *115*, 4312; *Angew. Chem. Int. Ed.* **2003**, *42*, 4180–4183.
- [8] a) A. Müller, E. Krickemeyer, H. Bögge, M. Schmidtman, F. Peters, *Angew. Chem. Int. Ed.* **1998**, *37*, 3360–3363; b) A. Müller, E. Krickemeyer, J. Meyer, H. Bögge, F. Peters, W. Plass, E. Diemann, S. Dillinger, F. Nonnenbruch, M. Randerath, C. Menke, *Angew. Chem.* **1995**, *107*, 2293; *Angew. Chem. Int. Ed. Engl.* **1995**, *34*, 2122–2124; c) A. Müller, E. Krickemeyer, H. Bögge, M. Schmidtman, C. Beugholt, P. Kögerler, C. Lu, *Angew. Chem.* **1998**, *110*, 1278; *Angew. Chem. Int. Ed.* **1998**, *37*, 1220–1223; d) C.-C. Jiang, Y.-G. Wei, Q. Liu, S.-W. Zhang, M.-C. Shao, Y.-Q. Tang, *Chem. Commun.* **1998**, 1937–1938; e) A. Müller, E. Beckmann, H. Bögge, M. Schmidtman, A. Dress, *Angew. Chem.* **2002**, *114*, 1210; *Angew. Chem. Int. Ed.* **2002**, *41*, 1162–1167; f) A. Müller, B. Botar, S. K. Das, H. Bögge, M. Schmidtman, A. Merca, *Polyhedron* **2004**, *23*, 2381–2385.
- [9] a) H. N. Miras, G. J. T. Cooper, D.-L. Long, H. Bögge, A. Müller, C. Streb, L. Cronin, *Science* **2010**, *327*, 72–74; b) H. N. Miras, D.-L. Long, P. Kögerler, L. Cronin, *Dalton Trans.* **2008**, 214–221; c) H. N. Miras, J. Yan, D.-L. Long, L. Cronin, *Angew. Chem.* **2008**, *120*, 8548; *Angew. Chem. Int. Ed.* **2008**, *47*, 8420–8423; d) N. G. Armatas, W. Ouellette, K. Whitenack, J. Pelcher, H. Liu, E. Romaine, C. J. O'Connor, J. Zubieta, *Inorg. Chem.* **2009**, *48*, 8897–8910; e) H. Tan, Y. Li, Z. Zhang, C. Qin, X. Wang, E. Wang, Z. Su, *J. Am. Chem. Soc.* **2008**, *130*, 10066–10067; f) L. Lisnard, P. Mialane, A. Dolbecq, J. Marrot, J. M. Clemente-Juan, E. Coronado, B. Keita, P. de Oliveira, L. Nadjo, F. Sécheresse, *Chem. Eur. J.* **2007**, *13*, 3525–3536.
- [10] a) S. Shishido, T. Ozeki, *J. Am. Chem. Soc.* **2007**, *129*, 10588–10595; b) B. Botar, P. Kögerler, C. L. Hill, *J. Am. Chem. Soc.* **2006**, *128*, 5336–5337.
- [11] a) R. Bhattacharyya, P. K. Chakrabarty, P. N. Ghosh, A. K. Mukherjee, D. Podder, M. Mukherjee, *Inorg. Chem.* **1991**, *30*, 3948–3955; b) A. Müller, E. Diemann, R. Jostes, H. Bögge, *Angew. Chem.* **1981**, *93*, 957; *Angew. Chem. Int. Ed. Engl.* **1981**, *20*, 934–955; c) H. N. Miras, J. D. Woollins, A. M. Slawin, R. Raptis, P. Baran, T. A. Kabanos, *Dalton Trans.* **2003**, 3668–3670; d) E. Cadot, B. Salignac, S. Halut, F. Sécheresse, *Angew. Chem. Int. Ed.* **1999**, *38*, 611–613.
- [12] T. Shibahara, *Coord. Chem. Rev.* **1993**, *123*, 73–147.
- [13] D. Coucouvanis, A. Toupadakis, J. D. Lane, S. M. Koo, C. G. Kim, A. Hadjikyriakou, *J. Am. Chem. Soc.* **1991**, *113*, 5271–5282.
- [14] A. Müller, R. Jostes, W. Elztner, C. S. Nie, E. Diemann, H. Bögge, M. Zimmermann, M. Dartmann, U. Reinsch-Vogell, S. Che, S. J. Cyvin, B. N. Cyvin, *Inorg. Chem.* **1985**, *24*, 2872–2884.
- [15] F. Sécheresse, S. Bernés, F. Robert, Y. Jeannin, *Bull. Soc. Chim. Fr.* **1995**, *132*, 1029–1037.
- [16] K. Hegetschweiler, T. Keller, H. Zimmermann, W. Schneider, H. Schmalte, E. Dubler, *Inorg. Chim. Acta* **1990**, *169*, 235–243.
- [17] A. Müller, U. Reinsch, *Angew. Chem.* **1980**, *92*, 69; *Angew. Chem. Int. Ed. Engl.* **1980**, *19*, 72–73.
- [18] V. P. Fedin, M. N. Sokolov, Yu. V. Minorov, B. A. Kolesov, S. V. Tkachev, V. Ye. Fedorov, *Inorg. Chim. Acta* **1990**, *167*, 39–45.
- [19] a) A. Kachmar, S. Floquet, J.-F. Lemonnier, E. Cadot, M.-M. Rohmer, M. Bénard, *Inorg. Chem.* **2009**, *48*, 6852–6859; b) E. Cadot, M.-A. Pilette, J. Marrot, F. Sécheresse, *Angew. Chem.* **2003**, *115*, 2223; *Angew. Chem. Int. Ed.* **2003**, *42*, 2173–2176; c) F. Sécheresse, E. Cadot, C. Simonnet-Jegat, in *Metal Clusters in Chemistry* (Eds.: P. Braunstein, L. A. Oro, P. R. Raithby), Wiley-VCH, Weinheim, Germany, **2008**, vol. 1, pp. 124–142; d) E. Cadot, F. Sécheresse, *Chem. Commun.* **2002**, 2189–2197; e) E. Cadot, J. Marrot, F. Sécheresse, *Angew. Chem.* **2001**, *113*, 796; *Angew. Chem. Int. Ed.* **2001**, *40*, 774–777; f) C. du Peloux, A. Dolbecq, P. Barboux, G. Laurent, J. Marrot, F. Sécheresse, *Chem. Eur. J.* **2004**, *10*, 3026–3032.
- [20] a) V. S. Korenev, A. G. Boulay, A. Dolbecq, M. N. Sokolov, A. Hijazi, S. Floquet, V. P. Fedin, E. Cadot, *Inorg. Chem.* **2010**, *49*, 9740–9742; b) A. Dolbecq, E. Cadot, F. Sécheresse, *Chem. Commun.* **1998**, 2293–2294.
- [21] H. N. Miras, E. F. Wilson, L. Cronin, *Chem. Commun.* **2009**, 1297–1311.
- [22] a) D.-L. Long, C. Streb, Y.-F. Song, S. Mitchell, L. Cronin, *J. Am. Chem. Soc.* **2008**, *130*, 1830–1832; b) H. N. Miras, D. J. Stone, E. J. L. McInnes, R. G. Raptis, P. Baran, G. I. Chilas, M. P. Sigalas, T. A. Kabanos, L. Cronin, *Chem. Commun.* **2008**, 4703–4705.
- [23] a) Y.-F. Song, D.-L. Long, S. E. Kelly, L. Cronin, *Inorg. Chem.* **2008**, *47*, 9137–9139; b) H. N. Miras, M. N. C. Ochoa, D.-L. Long, L. Cronin, *Chem. Commun.* **2010**, *46*, 8148–8150; c) R. Tsunashima, D.-L. Long, H. N. Miras, D. Gabb, C. P. Pradeep, L. Cronin, *Angew. Chem. Int. Ed.* **2010**, *49*, 113–116.
- [24] D.-L. Long, Y.-F. Song, E. F. Wilson, P. Kögerler, S.-X. Guo, A. M. Bond, J. S. J. Hargreaves, L. Cronin, *Angew. Chem.* **2008**, *120*, 4456; *Angew. Chem. Int. Ed.* **2008**, *47*, 4384–4387.
- [25] a) E. F. Wilson, H. Abbas, B. J. Duncombe, C. Streb, D.-L. Long, L. Cronin, *J. Am. Chem. Soc.* **2008**, *130*, 13876–13884; b) L. Vilà-Nadal, A. Rodríguez-Fortea, L.-K. Yan, E. F. Wilson, L. Cronin, J. M. Poblet, *Angew. Chem.* **2009**, *121*, 5560; *Angew. Chem. Int. Ed.* **2009**, *48*, 5452–5456; c) D. K. Walanda, R. C. Burns, G. A. Lawrence, E. I. von Nagy-Felsobuki, *J. Chem. Soc., Dalton Trans.* **1999**, *3*, 311–321.
- [26] V. P. Fedin, B. A. Kolesov, Yu. V. Mironov, A. Gerasko, V. Ye. Fedorov, *Polyhedron* **1991**, *10*, 997–1005.
- [27] E. Cadot, B. Salignac, S. Halut, F. Sécheresse, *Angew. Chem. Int. Ed.* **1999**, *38*, 611–613.
- [28] E. Cadot, B. Salignac, J. Marrot, A. Dolbecq, F. Sécheresse, *Chem. Commun.* **2000**, 261–262.
- [29] V. S. Korenev, A. G. Boulay, A. Dolbecq, M. N. Sokolov, A. Hijazi, S. Floquet, V. P. Fedin, E. Cadot, *Inorg. Chem.* **2010**, *49*, 9740–9742.
- [30] a) L. Seguin, M. Figlarz, R. Cavagnat, J.-C. Lassegues, *Spectrochim. Acta Part A* **1995**, *51*, 1323–1344; b) K. Eda, N. Sotani, *Bull. Chem. Soc. Jpn.* **1989**, *62*, 4039.
- [31] a) X. Du, L. Dong, C. Li, Y. Liang, Y. Chen, *Langmuir* **1999**, *15*, 1693–1698; b) M. A. Py, K. Maschke, *Phys. B* **1981**, *105*, 370–374.
- [32] a) G. A. Narzri, C. Julien, *Solid State Ionics* **1992**, *53–56*, 376; b) C. Julien, G. A. Narzri, *Solid State Ionics* **1994**, *68*, 111.
- [33] K. H. Tytko, B. Schönfeld, B. Buss, O. Glemser, *Angew. Chem.* **1973**, *85*, 305; *Angew. Chem. Int. Ed. Engl.* **1973**, *12*, 330–332.
- [34] M. T. Pope, A. Müller (Eds.), *Polyoxometalate Chemistry: From Topology via Self-Assembly to Applications*, Kluwer Academic Publishers, Dordrecht, The Netherlands, **2001**.
- [35] N. B. Librovich, V. P. Sakun, N. D. Sokolov, *Chem. Phys.* **1979**, *39*, 351–366.
- [36] H. Abramczyk, *Chem. Phys.* **1990**, *144*, 305–318.
- [37] A. Müller, E. Krickemeyer, U. Reinsch, *Z. Anorg. Allg. Chem.* **1980**, *470*, 35–38.
- [38] G. M. Sheldrick, *Acta Crystallogr., Sect. A* **1990**, *46*, 467–473.
- [39] G. M. Sheldrick, *SHELXL-97, Program for Crystal structure analysis*, University of Göttingen, Germany, **1997**.
- [40] L. J. Farrugia, *J. Appl. Crystallogr.* **1999**, *32*, 837–838.

Received: August 8, 2011

Published Online: October 18, 2011